



Structure Modification Of MoS₂ Through Preparation Condition Management

H. H. Afify¹, M. Obaida¹, Mai N. Swelam^{1*}, S.A. Hassan¹, H. M. Hashem², A. abd El-Mongy²

¹Solid State Physics Department, Physics Research Institute, National Research Centre, 33 El Buhouth St., Dokki, 12622 Giza, Egypt

²Physics Department, Faculty of Science, Helwan University, Cairo, Egypt



Abstract

The structure of the final product 2D-MoS₂ is modified through preparation conditions modulation. One pot simple and easy procedure hydrothermal technique is used for MoS₂ powder preparation. The precursor solution pH is varied in the acidic side from 1 up to 5. The reaction temperature and time in the autoclave are kept constant while the pH is varied. The change in pH is studied at each of two reaction temperature 210°C & 230°C and each one of three reaction time 24, 48, 72 hour. Crystal structure and phase identification are elucidated by XRD measurements. Morphology, shape and size of fine structures are demonstrated by FESEM & HRTEM images. As well surface area, elemental analysis and oxidation state of elements are explored by BET, EDX and XPS measuring technique. XRD patterns peaks of the investigated sample are indexed with JCPDS standard files and found to be well matched with that of 2H-MoS₂ phase of MoS₂ product. Also the crystallite size is calculated by Applying SHERER equation on the well define and high intensity peak in XRD pattern. XRD patterns show that at both low reaction time and temperature the end product is almost amorphous at PH 1&3 while at 4&5 it is poly crystalline. FESEM micrographs show flower-like structure composed of spheres of nanosheets. HRTEM images demonstrate more details about the present fine structures such as Nano sheet spheres and their arrangement. As well SAED patterns identified the amorphous and crystalline state combined with nomination of planes. Also, the arrangement of Nano sheets and distance between layers in the bundle are determined. Surface area of MoS₂ constituents is measured by BET method. The obtained results show that samples with (001) plane have value 59m²/g while that contain (002) plane have value 19m²/g. The elemental analysis measured by EDX display the existed elements S & Mo with their percentage. The ratio of Mo/S is found to be nearly 1/2. The existed elements of MoS₂ product is confirmed by XPS measurements with the oxidation state of the elements are determined from Mo & S peaks and their deconvolution.

Keywords: MoS₂; Hydrothermal method; Crystal growth; Nanocrystalline materials; Microstructure.

1. Introduction

Transition-metal chalcogenides (TMDCs) have a promising future so researchers have put a large focus on their studying and low cost preparation. Chemical formula of TMDCs is MX₂ where M referred to the transition-metals (M = Ti, Zr, Hf, V, Nb, Ta, Mo, W, Pt) and X is referred to the chalcogens (X = S, Se, Te) [1-4]. TMDs can be semiconductors, true metals, semi-metals, or superconductors depending on their composition[5]. In monolayer TMDC, the transition-metal atoms are sandwiched between two chalcogen atoms [6]. Like graphene, TMDCs have a strong in-plane covalent bond and weak van der Waals between layers also the properties of TMDCs change with the thickness. TMDCs in bulk semiconducting form have an indirect bandgap. While in several layer form have a direct bandgap [5].

TMDCs are excellent for electronic devices like transistors, photodetectors .., etc. because of their shift from indirect to direct bandgap from bulk to single layer respectively. Also, TMDCs have been used in other applications, for example, photovoltaics, lithium-ion batteries, and ultrasensitive biosensors just to name a few. [7,8].

Molybdenum disulfide (MoS₂) is one of the transitional materials chalcogenides (TMDCs) with an X-M-X structure. MoS₂ is usually crystallized in three different structures 2H, 3R, and 1T. where 2H-MoS₂ (two-layer hexagonal) and 3R-MoS₂ (three-layer rhombohedral) are the stable phases that can be exist for Bulk MoS₂[9]. Moreover 2H is the most common and stable phase among these three. Also, both 1T and 3R phases can change to 2H structure through heating. 2H-MoS₂ unit cells consist of two

*Corresponding author e-mail: mn.swelam@nrc.sci.eg

Receive Date: 27 February 2022, Revise Date: 09 March 2022, Accept Date: 14 March 2022

DOI: 10.21608/EJCHEM.2022.124371.5540

©2022 National Information and Documentation Center (NIDOC)

tri-atomic layers which are centrosymmetric to each other, creating hexagonal structure. The layers are connected by weak van der Waals force, which enables the easy intercalation of hetero-molecules[10,11]. However, the atoms within a layer are connected by strong covalent forces. This high anisotropy crystal structure results in two types of exposed surfaces: (002) planes along the edges of S-Mo-S (c axis) named as basal planes and (100) planes along the edges of S-Mo named as edges. Theoretical researches and experimental results reveal that the basal planes are inert and stable, thus the edges, especially the sulfur edge- terminated edges serve as active sites for many important catalytic reactions, such as hydrogen evolution reactions (HER) in electrochemistry[12], hydrogenation[2] and hydro-desulfurization (HDS)[13]. Furthermore MoS₂ flakes have been deployed in the development of gas sensors[14-17] and have demonstrated good ability for sensing[18].

Herein, it is focused on low cost preparation of typical single phase 2H-MoS₂ with interlayer distance 0.64nm and development of it to be with wide interlayer spacing 0.94nm. The characterizing measurement techniques such as XRD, FESEM, HRTEM, BET, EDX and XPS are performed to explore the nature of the prepared end product.

2. Experimental Details

2.1 synthesis of MoS₂ (hydrothermal technique):

The Purchased Materials Ammonium molybdate tetrahydrate (NH₄)₆Mo₇O₂₄.4H₂O and thiourea NH₂CSNH₂ with purity 99.5% as a source of Mo and S are used as received without any treatment. Distilled water is used as a solvent. The precursor solution is prepared by dissolving 2.48 gm of (NH₄)₆Mo₇O₂₄.4H₂O and 4.56 gm thiourea NH₂CSNH₂ into 70mL de-ionized water

The mixed precursor solution 70mL is poured into 100mL Teflon lined stainless steel autoclave. The precursor solution pH is adjusted by adding drops of HCl to be 1, 3, 4 & 5. Then the autoclave transferred directly to a furnace adjusted at the required temperature and staying time. After reaching the required time the furnace power is turned off and leaved to cool naturally at room temperature. Both reaction time and temperature are varied to be 24h, 48h, 72h and 200°C, 210°C & 230°C, respectively. At each constant time and temperature of these the pH is changed from 1 up to 5. At the end the final product is washed thoroughly several times by water and ethanol then dried at 60°C for 5 hours. The samples are classified to groups according to reaction temperature T_c, time t_h and pH value.

The variation effect of precursor solution pH 1,3,4,5 on MoS₂ growth is studied at each of the three constant reaction time 24h, 48h & 72h and each of

the two constant reaction temperature 210°C & 230°C. The effect of reaction time 24h, 48h & 72h is investigated on samples prepared at each of the two pH 1, 5. As well the effect of reaction temperature is studied at constant pH 5 and each of the two reaction time 24h & 48h.

3. Result and discussion

3.1. X-Ray Diffraction - Structural analysis

I) Effect of precursor solution pH

All samples are examined by X-ray diffraction XRD to identify crystalline nature, present phases and crystallite size. The obtained XRD patterns for samples prepared at each one of the two constant reaction temperature 210°C & 230°C and each constant reaction time 24h, 48h & 72h at varied pH (1, 3, 4 & 5) are demonstrated by Fig.1 (a, b, c) and Fig.2 (a, b, c). It is salient from Fig.1 (a) that samples with pH (1 & 3) are mostly amorphous since their patterns are empty from any clear peak corresponding to any formed plane in the MoS₂ ordered structure. On contrast those samples with pH (4 & 5) show 4 peaks at 2θ = 9.5°, 18.5°, 33° & 58° which correspond to (001), (003), (100) & (110) respectively which indicate polycrystalline nature. By indexing these peaks with JCPDS files well match with the file no #73-1508 corresponding to 2H-MoS₂ phase is found. All XRD patterns are totally empty from any peak corresponding to any impurity or other phases related MoS₂. The existence of (001) & (003) emphasize layer structure via c-axis. When the reaction time increased to 48h all peaks characterizing 2H-MoS₂ phase are appeared regardless the P^H value which means that the samples have the same atomic arrangement but with poor crystallinity as indicated by low intensity of peaks Fig.1(b). It is worth to note that the (002) identifying typical 2H-MoS₂ phase with ordered stacking layers spaced by 0.63nm is absent in XRD patterns of samples have reaction time 24h & 48h while it appears when the reaction time increased to 72h. This means that when the reaction time <72h the formed 2H-MoS₂ phase has layer structure with wide distance 0.94nm between the stacked layers as deduced from appearance of clear and defined peak at 2θ = 9.5° corresponding to (001). This finding is reported in few papers using some additives in their hydrothermal preparation [1, 3].

There When both reaction temperature and time increased to 230°C and 48h respectively all characteristic peaks of 2H-MoS₂ except that at 2θ = 14. All peaks have relatively lower intensity excluding that at 2θ = 9.5° corresponding to (001) which has higher intensity irrespective to pH values. The XRD patterns looks like that for epitaxial growth since only one plane of growth is present which indicate preferred orientation growth. The variation

effect of precursor solution P^{H} is significantly observed only for samples prepared at both reaction temperature (210°C) and time (24h). The crystallinity nature of the prepared samples changed from amorphous state at P^{H} 1&3 to crystalline state at pH (4 & 5).

The results of measuring surface area of samples have (001) & (002) plane by BET show significant difference in their values 53.5 & $19.5\text{m}^2/\text{g}$ which correspond to distance between layer stack 0.94nm & 0.63nm respectively.

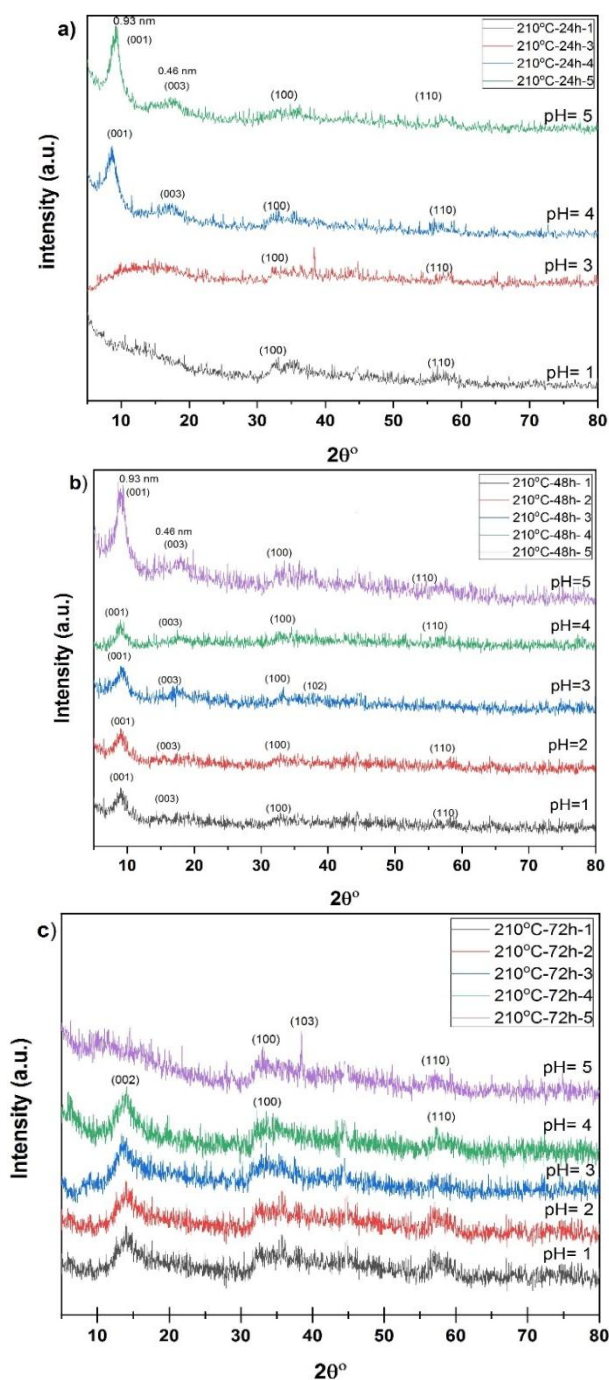


Fig.1 (a, b & c). XRD patterns of samples prepared at constant reaction temperature 210°C at different pH (1, 2, 3, 4 & 5) values and times (24, 48 & 72 h).

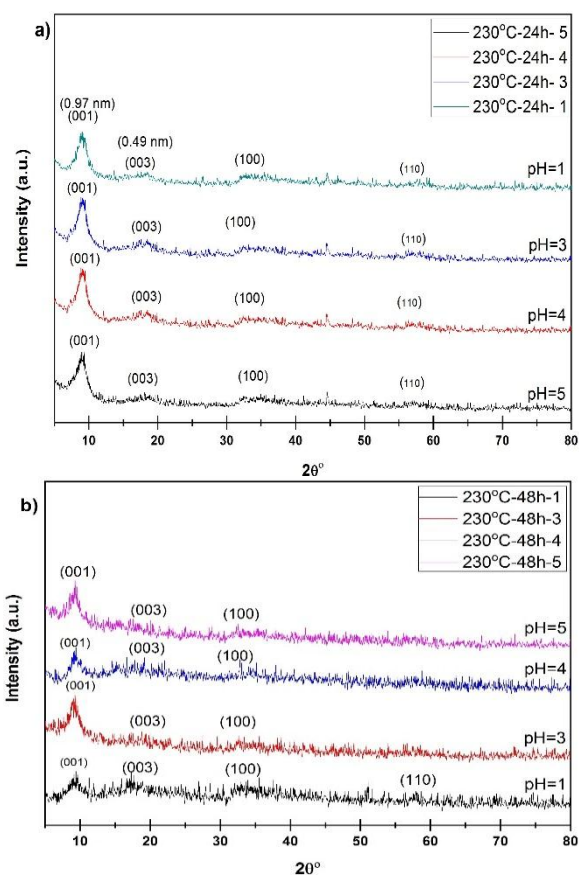


Fig. 2 (a, b). XRD patterns of samples prepared at constant reaction temperature 230°C at different pH (1, 2, 3, 4 & 5) values and times (24 & 48 h).

II) Effect of reaction temperature.

The XRD patterns of samples prepared at constant precursor pH 5 and constant reaction time 48h and different reaction temperatures 200°C , 210°C & 230°C are given in Fig. 3.

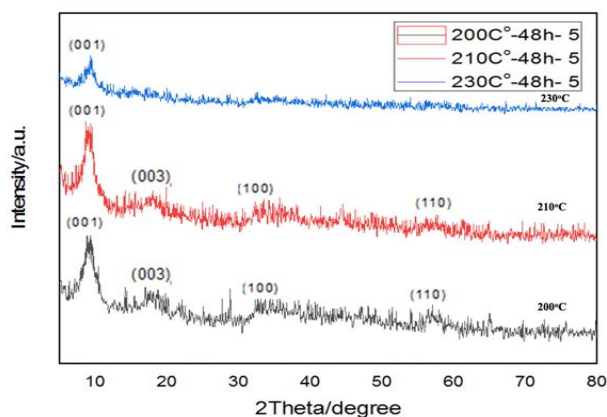


Fig. 3. XRD patterns of sample prepared at different reaction temperatures (200, 210 & 230°C) at constant pH 5 and time 48 h.

The change in reaction temperature has only an observable change in peak intensity corresponds to (001) plane. The increase in reaction temperature induces unobservable increase in (001) intensity at both 200°C & 210°C but at 230°C reasonable decrease

is noticed may be due to the onset of destroying the ordered atoms arrangement. This conjecture supported by vanish of all weak peaks at the high 2θ side. Obviously the (001) is the preferred orientation growth plane for samples prepared at 200°C & 210°C which indicates like epitaxial growth.

III) Effect of reaction time

As well the variation in reaction time is studied on samples prepared at constant pH 5 and temperature 210°C . Their XRD patterns is demonstrated in [Fig.4].

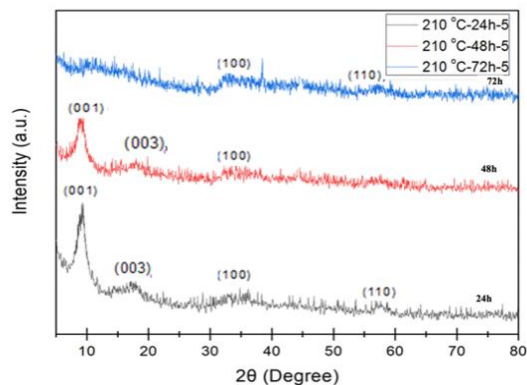


Fig. 4. XRD patterns of sample prepared at constant reaction temperature 210°C and pH 5 at different times (24, 48 & 72 h).

All peaks at high 2θ side corresponding to (003), (100) & (110) have too low intensity while that at $2\theta = 9.5^\circ$ has relatively high intensity which looks like epitaxial growth. The samples crystallinity decreases with increasing reaction time from 24h to 48h until it totally deteriorated at 72h. The effect of both reaction temperature and time, to great extent, are similar.

3.2. X-ray Photoelectron Spectroscopy (XPS) measurements - Structural analysis

The valence state of elements and elemental composition information of the final product were confirmed by the XPS spectra. In the case of samples that were prepared at constant pH 5 and preparation temperature 210°C and different time 24h, 48h and 72h (See fig. 5). Very strong Mo and S peaks corresponding to Mo 3d and S 2p can be seen at ~ 230 eV and ~ 162.9 eV, respectively. You will usually want to divide your article into (numbered) Fig. 5 (a, c & e) show a singlet structure centered at ~ 226 eV generated by photoelectrons emitted from the 2s core state of S atoms and a doublet structure by photoelectrons emitted from the 3d core state ($3d_{3/2}$ and $3d_{5/2}$ orbitals) of Mo atoms due to *l-s* coupling.

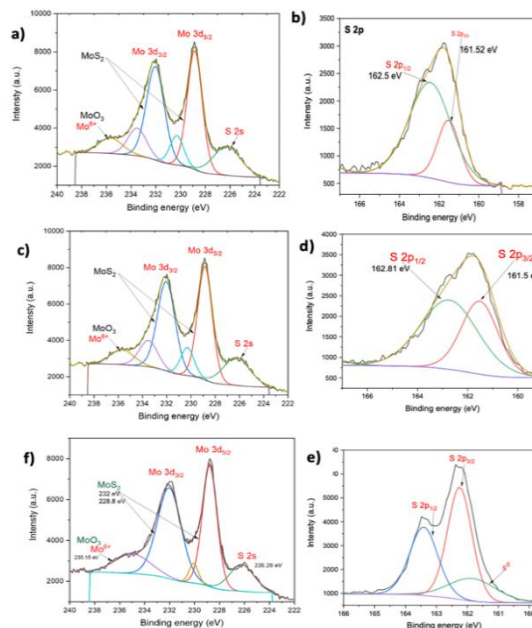


Fig 5: XPS spectra for samples prepared at constant pH 5 and preparation temperature 210°C and different time 24h, 48h and 72h. (a) high resolution spectra of Mo 3d peak doublet, (b) high resolution spectra of S 2p peak doublets.

The Mo $3d_{5/2}$ peak appears at ~ 228.8 eV while the Mo $3d_{3/2}$ peak appears at ~ 231.1 eV. The difference between the two peaks is ~ 3.2 eV for all samples, this confirms the presence of Mo in 4+ oxidation state necessary for the formation of MoS_2 [19-22]. also Mo^{6+} peak, which corresponds to the MoO_3 formation is also observed at ~ 235 eV [19]. Furthermore, the S 2p spectrum Fig. 5 (b, d & f) can be deconvoluted in two doublets ($2p_{1/2}$ and $2p_{3/2}$). The S $2p_{3/2}$ peak appears at ~ 161.5 eV while the S $2p_{1/2}$ peak appears at ~ 162.5 eV confirming the formation of sulfide [20,23]. The values of the binding energy confirm the formation of MoS_2 formation according to figure 5.

3.3. Field Emission Scanning Electron Microscope (FE-SEM) measurements with EDX - morphological analysis

FESEM images of the prepared samples at 210°C and pH 5 with various reaction time are shown in [Fig. 6 a -b-c]. The images represent sample prepared at 24h, 48h & 72h show nano sheets randomly oriented but at reaction time 48h a flower like structure composed of assembled nano sheets is prevails. The elemental analysis measured by Energy Dispersive X-Ray Analysis (EDX) for MoS_2 prepared at 24h, 48h & 72h listed in tables attached in Fig. 6 (d, e, f). The peaks related to the O, Mo and S elements are detected; no other elements are observed. Moreover, the ratio between Mo and S is $\sim 1:2$ in all samples prepared at 24h, 48h & 72h. However, the oxygen atomic percentage decrease with increasing reaction

time indicating release of oxygen at long reaction time.

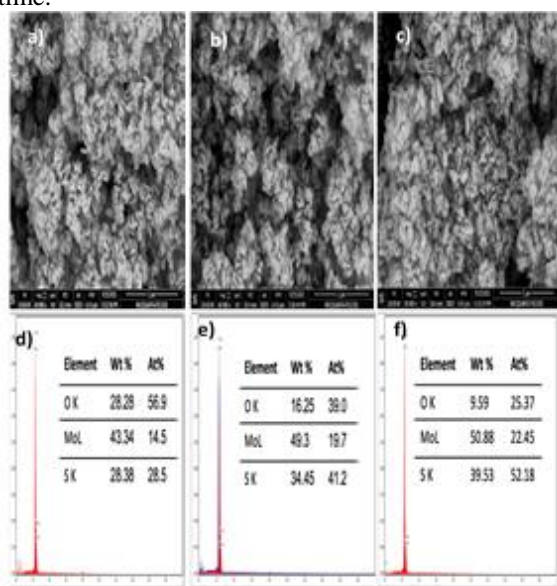


Fig. 6 (a, b & c) FE-SEM and (d, e & f) EDX graphs and elemental analysis tables images of samples prepared at constant pH5 and temperature 210°C at different reaction time (24h, 48h & 72h), respectively.

3.4. High-Resolution Transmission Electron Microscopy (HR-TEM) measurements - morphological analysis

Shape and size of substructures for MoS_2 combined with Selected Area Electron Diffraction SAED are examined by HRTEM. As prepared samples at 210°C and pH 5 with various reaction time are diagnosed by HRTEM. Low and high magnification HRTEM images for sample prepared at 24h, 48h & 72h combined with their SAED patterns are shown in Fig. 7. Low magnification images of samples prepared at 24h, 48h & 72h display elongated strips with average width 7.42nm assembled in bundles randomly distributed. Some of them gathered to form condensed Nano sheets while the others are crosslinked in sets of low number of strips with sharp edge and tapered end. Numbers not few of the strips are in individual state which increase the exposed surface area. The identity of preceding substructures is nearly similar for samples prepared at 24h, 48h & 72h reaction time.

Alternatively, high magnification images demonstrate bunch of long-term ordered sheets with interspace 0.26nm corresponding to (100) Fig. 7(b). Only one orientation of bundle comprise strips with ordered interlayer stack is clear. When the reaction time increased to 48h these bundles have different orientations with inter space layer 0.25nm Fig. 7(e). On contrary for samples prepared at 72h these bundles dissociated to be a singular elongated one widely separated from each other [Fig.7-h].

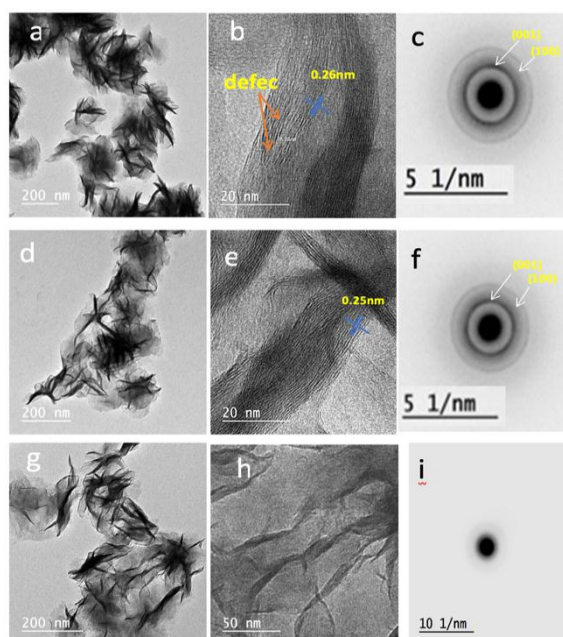


Fig. 7(a, b, d, e, g & h) HRTEM and (c, f & i) SAED patterns for samples prepared at constant pH5 and temperature 210°C at different reaction time (24h, 48h & 72h), respectively.

Selected Area Electron Diffraction SAED patterns for as prepared sample with 24h, 48h & 72h are given in Fig. 7(c, f & i). The SAED patterns for samples prepared at reaction time 24h & 48h display faint continuous rings correspond to planes (001) & (100) Fig. 7(c & f) proving low crystallinity. In contrast, the SAED pattern for sample with reaction time 72h is empty from any ring corresponding to plane existence Fig. 7(i) which indicate sample amorphicity and/or amorphous phase prevailing on crystalline phase.

Conclusions

The present work deals with studying the preparation and characterization of MoS_2 . Hydrothermal technique is used to prepare MoS_2 on one shot since it is simple, low cost and easy to operate. pH, both reaction temperature and time are managed to obtain layered pure single phase 2H- MoS_2 with different interlayer distance. The pH is varied from 1 up to 5 while both reaction temperature and time are constant. As well, effect of reaction temperature is studied at constant pH 5 and reaction time 48h. Also the effect of reaction time is diagnosed at constant pH 5 and reaction temperature 210°C . The end product MoS_2 at each of the preceding conditions is subjected to characterizing measurements such as XRD, FESEM, EDX, HRTEM and XPS.

The change of pH has significant effect at both low reaction temperature and time. The samples are amorphous at pH 1 & 3 and polycrystalline at pH 4 & 5. All crystalline samples have preferred orientation and look like epitaxial growth. Single 2H- MoS_2

phase is prepared with typical interlayer distance 0.64nm and wide space between layers 0.94nm. An interesting peak at $2\theta = 9.4^\circ$ with reasonable intensity and broadening is observed in all preparation conditions except those at reaction time 72h. This peak is not recorded in JCPDS files but observed by several authors. The detailed morphological nature is explored by FESEM and HRTEM while crystalline nature by SAED. Flower-like MoS₂ microspheres have been synthesized, it was found that the prepared MoS₂ microspheres were constructed by MoS₂ nanosheets randomly oriented with stacked layered structure. The elemental analysis is determined by both EDX & XPS. The ratio of Mo/S is found to be nearly 1/2. The traditional and typical 2H-MoS₂ pure single phase with a wide interlayer space which is very important in water pollutant removal and photocatalytic reactions are successfully prepared.

3. Conflicts of interest

There are no conflicts to declare.

4. Formatting of funding sources

List funding sources in a standard way to facilitate compliance to funder's requirements.

5. Acknowledgments

Deep thanks to Prof. G. M. Elkomy, Department of Electron Microscopes and Thin Film, National Research Centre for her valuable guidance and support.

6. References

- [1] L. Ma, L.-M. Xu, X.-P. Zhou, and X.-Y. Xu, "Biopolymer-assisted hydrothermal synthesis of flower-like MoS₂ microspheres and their supercapacitive properties," *Mater. Lett.*, vol. 132, pp. 291–294, 2014.
- [2] M. Li *et al.*, "Facile hydrothermal synthesis of MoS₂ nano-sheets with controllable structures and enhanced catalytic performance for anthracene hydrogenation," *RSC Adv.*, vol. 6, no. 75, pp. 71534–71542, 2016.
- [3] M. R. Saber, G. Khabiri, A. A. Maarouf, M. Ulbricht, and A. S. G. Khalil, "A comparative study on the photocatalytic degradation of organic dyes using hybridized 1T/2H, 1T/3R and 2H MoS₂ nano-sheets," *RSC Adv.*, vol. 8, no. 46, pp. 26364–26370, 2018.
- [4] D. Jariwala, V. K. Sangwan, L. J. Lauhon, T. J. Marks, and M. C. Hersam, "Emerging device applications for semiconducting two-dimensional transition metal dichalcogenides," *ACS Nano*, vol. 8, no. 2, pp. 1102–1120, 2014.
- [5] R. Lv *et al.*, "Transition metal dichalcogenides and beyond: synthesis, properties, and applications of single- and few-layer nanosheets," *Acc. Chem. Res.*, vol. 48, no. 1, pp. 56–64, 2015.
- [6] Y.-H. Wang, K.-J. Huang, and X. Wu, "Recent advances in transition-metal dichalcogenides based electrochemical biosensors: A review," *Biosens. Bioelectron.*, vol. 97, pp. 305–316, 2017.
- [7] Q. H. Wang, K. Kalantar-Zadeh, A. Kis, J. N. Coleman, and M. S. Strano, "Electronics and optoelectronics of two-dimensional transition metal dichalcogenides," *Nat. Nanotechnol.*, vol. 7, no. 11, pp. 699–712, 2012.
- [8] F. Schwierz, J. Pezoldt, and R. Granzner, "Two-dimensional materials and their prospects in transistor electronics," *Nanoscale*, vol. 7, no. 18, pp. 8261–8283, 2015.
- [9] R. Suzuki *et al.*, "Valley-dependent spin polarization in bulk MoS₂ with broken inversion symmetry," *Nat. Nanotechnol.*, vol. 9, no. 8, pp. 611–617, 2014.
- [10] E. Benavente, M. A. Santa Ana, F. Mendizábal, and G. González, "Intercalation chemistry of molybdenum disulfide," *Coord. Chem. Rev.*, vol. 224, no. 1–2, pp. 87–109, 2002.
- [11] C. Tsai, K. Chan, J. K. Nørskov, and F. Abild-Pedersen, "Rational design of MoS₂ catalysts: tuning the structure and activity via transition metal doping," *Catal. Sci. Technol.*, vol. 5, no. 1, pp. 246–253, 2015.
- [12] X. Xu and L. Liu, "MoS₂ with controlled thickness for electrocatalytic hydrogen evolution," *Nanoscale Res. Lett.*, vol. 16, no. 1, pp. 1–10, 2021.
- [13] C. Rong and X. Qin, "Quantum chemical study of MoS₂ hydro desulfurization catalysts," *J. Mol. Catal.*, vol. 64, no. 3, pp. 321–335, 1991.
- [14] D. Wu *et al.*, "Construction of MoS₂/Si nanowire array heterojunction for ultrahigh-sensitivity gas sensor," *Nanotechnology*, vol. 28, no. 43, p. 435503, 2017.
- [15] G. Liu, S. L. Rumyantsev, C. Jiang, M. S. Shur, and A. A. Balandin, "Selective Gas Sensing With h -BN Capped MoS₂ Heterostructure Thin-Film Transistors," *IEEE Electron Device Lett.*, vol. 36, no. 11, pp. 1202–1204, 2015.
- [16] A. Shokri and N. Salami, "Gas sensor based on MoS₂ monolayer," *Sensors Actuators B Chem.*, vol. 236, pp. 378–385, 2016.
- [17] H. Yan, P. Song, S. Zhang, J. Zhang, Z. Yang, and Q. Wang, "A low temperature gas sensor based on Au-loaded MoS₂ hierarchical nanostructures for detecting ammonia," *Ceram. Int.*, vol. 42, no. 7, pp. 9327–9331, 2016.
- [18] Q. Zhou *et al.*, "Hierarchically MoS₂ nanospheres assembled from nanosheets for superior CO gas-sensing properties," *Mater. Res. Bull.*, vol. 101, pp. 132–139, 2018.

- [19] M. A. Hossain, B. A. Merzougui, F. H. Alharbi, and N. Tabet, "Electrochemical deposition of bulk MoS_2 thin films for photovoltaic applications," *Sol. Energy Mater. Sol. Cells*, vol. 186, pp. 165–174, 2018.
- [20] L. Hu, Y. Ren, H. Yang, and Q. Xu, "Fabrication of 3D hierarchical MoS_2 /polyaniline and MoS_2/C architectures for lithium-ion battery applications," *ACS Appl. Mater. Interfaces*, vol. 6, no. 16, pp. 14644–14652, 2014.
- [21] G. Eda, H. Yamaguchi, D. Voiry, T. Fujita, M. Chen, and M. Chhowalla, "Photoluminescence from chemically exfoliated MoS_2 ," *Nano Lett.*, vol. 11, no. 12, pp. 5111–5116, 2011.
- [22] W. Gu, Y. Yan, C. Zhang, C. Ding, and Y. Xian, "M.A. Hossain, B.A. Merzougui, F.H. Alharbi, N. Tabet, Electrochemical deposition of bulk MoS_2 thin films for photovoltaic applications, Sol. Energy Mater.," *ACS Appl. Mater. Interfaces*, vol. 8, no. 18, pp. 11272–11279, 2016.
- [23] W. Gu, Y. Yan, C. Zhang, C. Ding, and Y. Xian, "One-step synthesis of water-soluble MoS_2 quantum dots via a hydrothermal method as a fluorescent probe for hyaluronidase detection," *ACS Appl. Mater. Interfaces*, vol. 8, no. 18, pp. 11272–11279, 2016.